Electronic Supplementary Material (ESI) for Journal of Materials Chemistry A.

Supporting Information

Co-prosperity of electrocatalytic activity and stability in high entropy spinel $(Cr_{0.2}Mn_{0.2}Fe_{0.2}Ni_{0.2}Zn_{0.2})_3O_4$ for oxygen evolution reaction

Xu Yang, Sun Liping*, Li Qiang, Huo Lihua, Zhao Hui*

Key Laboratory of Functional Inorganic Material Chemistry, Ministry of Education, School of Chemistry and Materials Science, Heilongjiang University, Harbin 150080, P. R. China

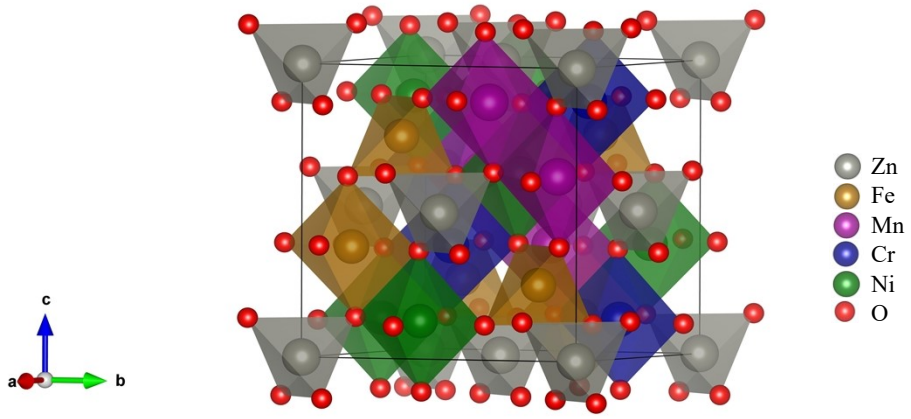

Fig. S1 Structure model of the high entropy spinel oxide $(Cr_{0.2}Mn_{0.2}Fe_{0.2}Ni_{0.2}Zn_{0.2})_3O_4$.

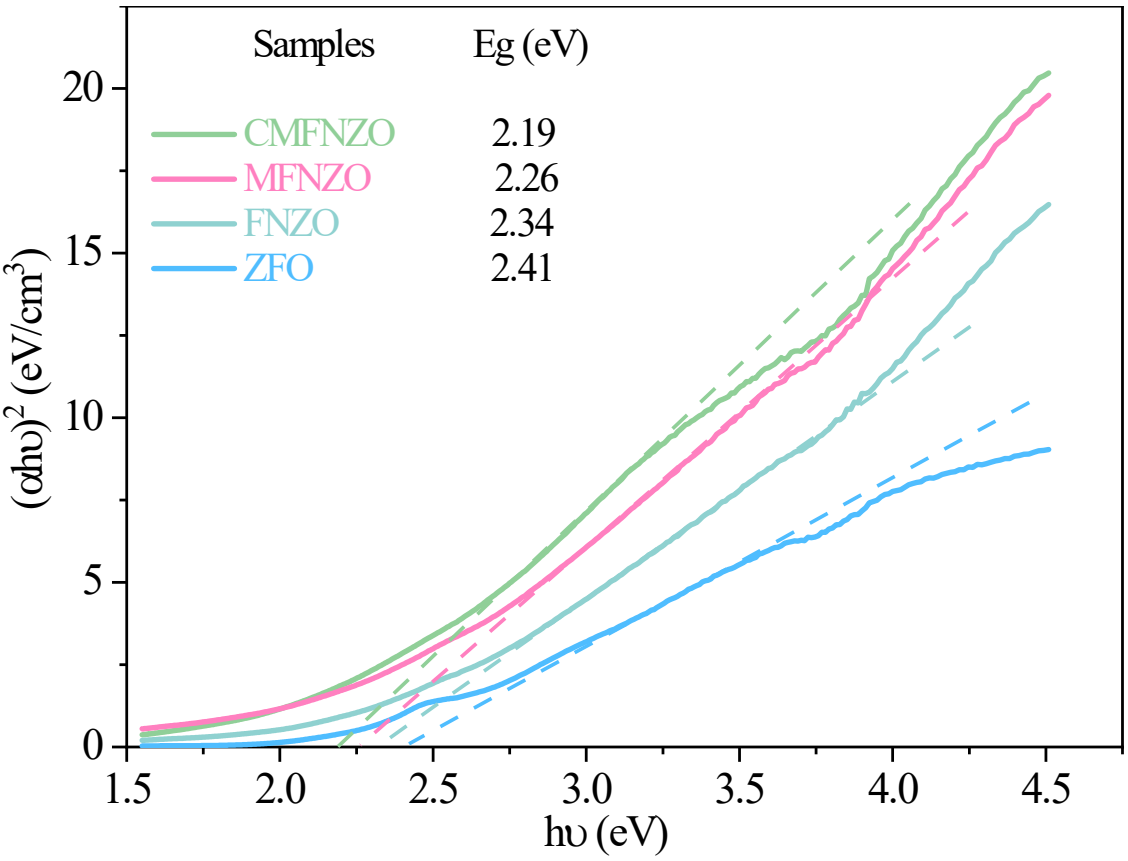

Fig. S2 The plot of $(\alpha h\nu)^2$ versus photon energy ($h\nu$).

The band gap energy (E_g) can be deduced from the relation $\alpha h\nu = C(h\nu - E_g)^{1/2}$

where α is the absorption coefficient, $h\nu$ is the photon energy, C is a constant, E_g is the band gap energy for direct transition.

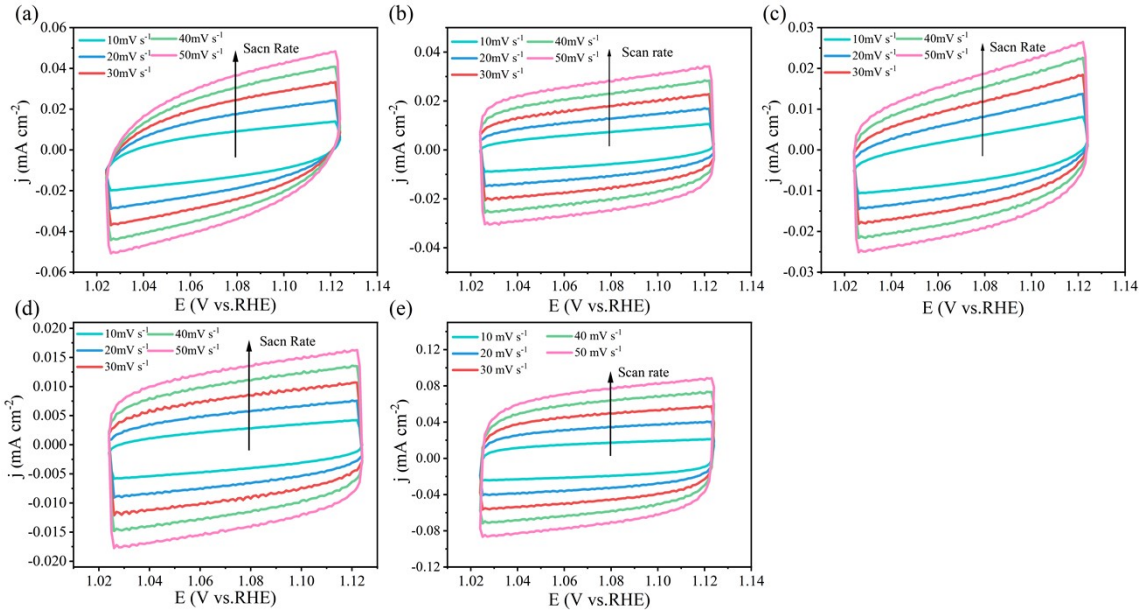

Fig. S3 The CV curves obtained at different scan rates of 10, 20, 30, 40 and 50 mV s^{-1} for (a) CMFNZO, (b) MFNZO, (c) FNZO, (d) ZFO and (e) RuO_2.

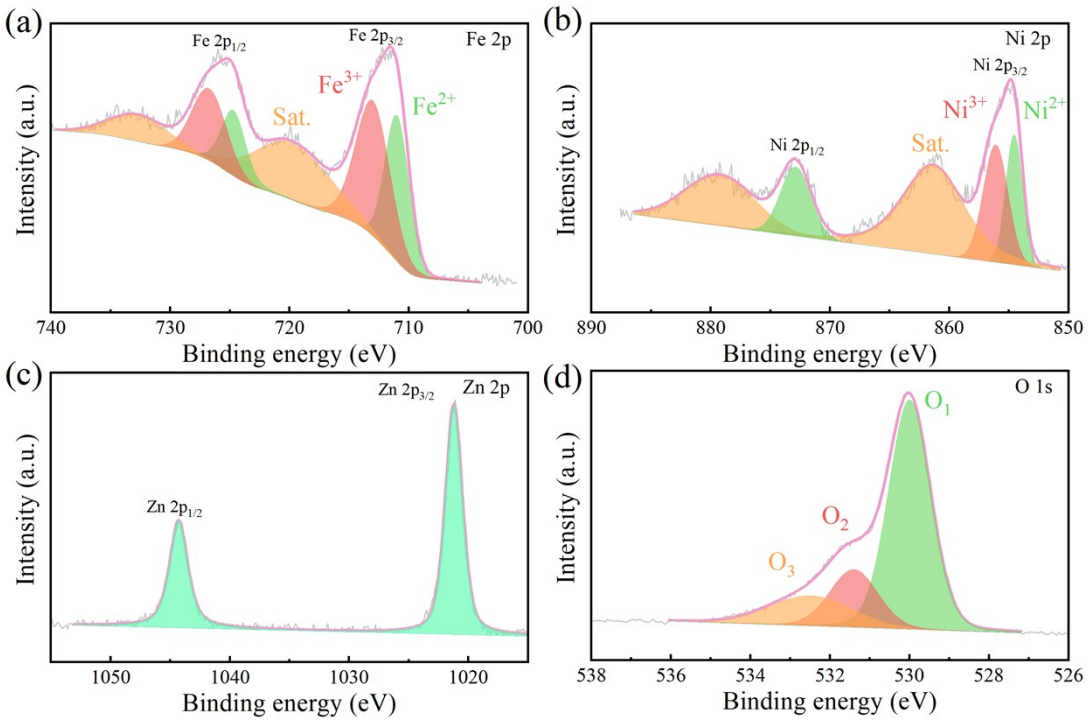

Fig. S4 XPS spectra for FNZO. (a) Fe 2p, (b) Ni 2p, (c) Zn 2p, (d) O 1s.

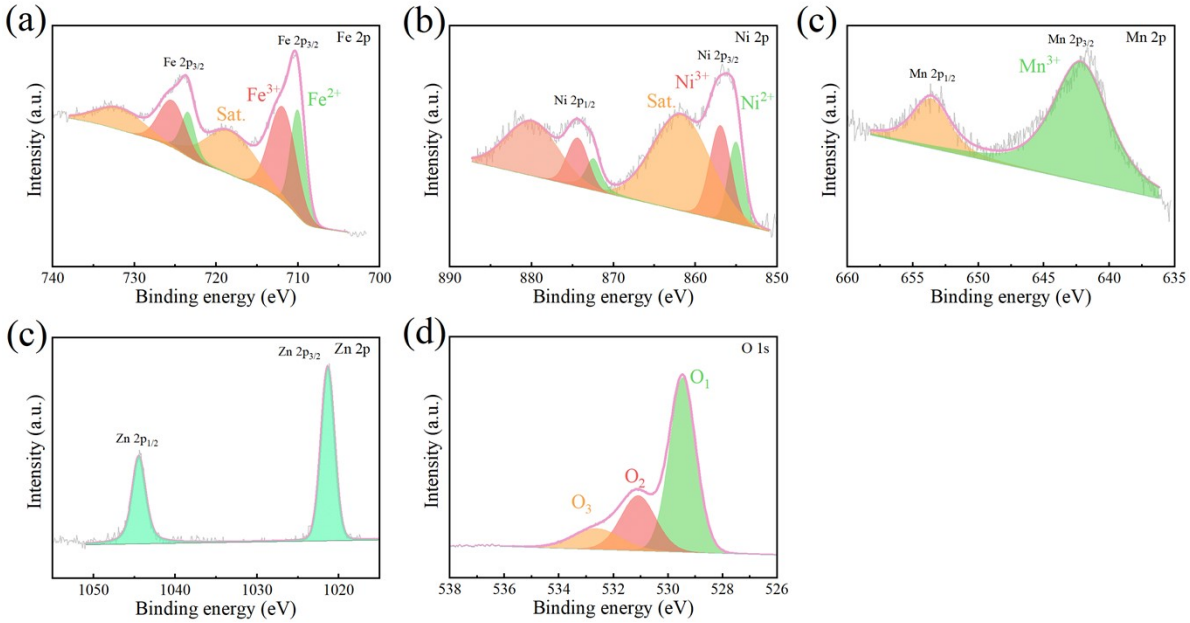

Fig. S5 XPS spectra for MFNZO. (a) Fe 2p, (b) Ni 2p, (c) Mn 2p, (d) Zn 2p, (e) O 1s.

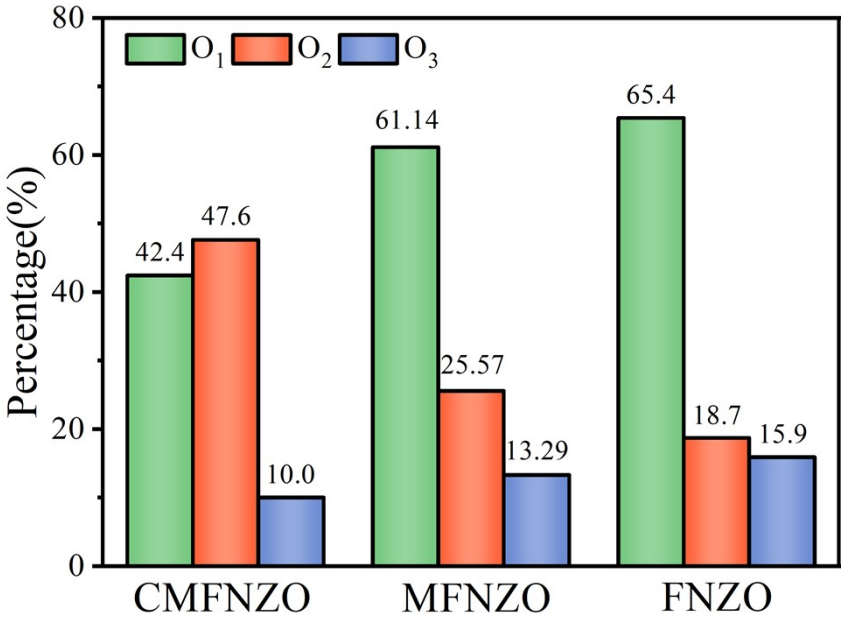

Fig. S6 Oxygen percentage of O_1, O_2, O_3 in CMFNZO, MFNZO and FNZO.

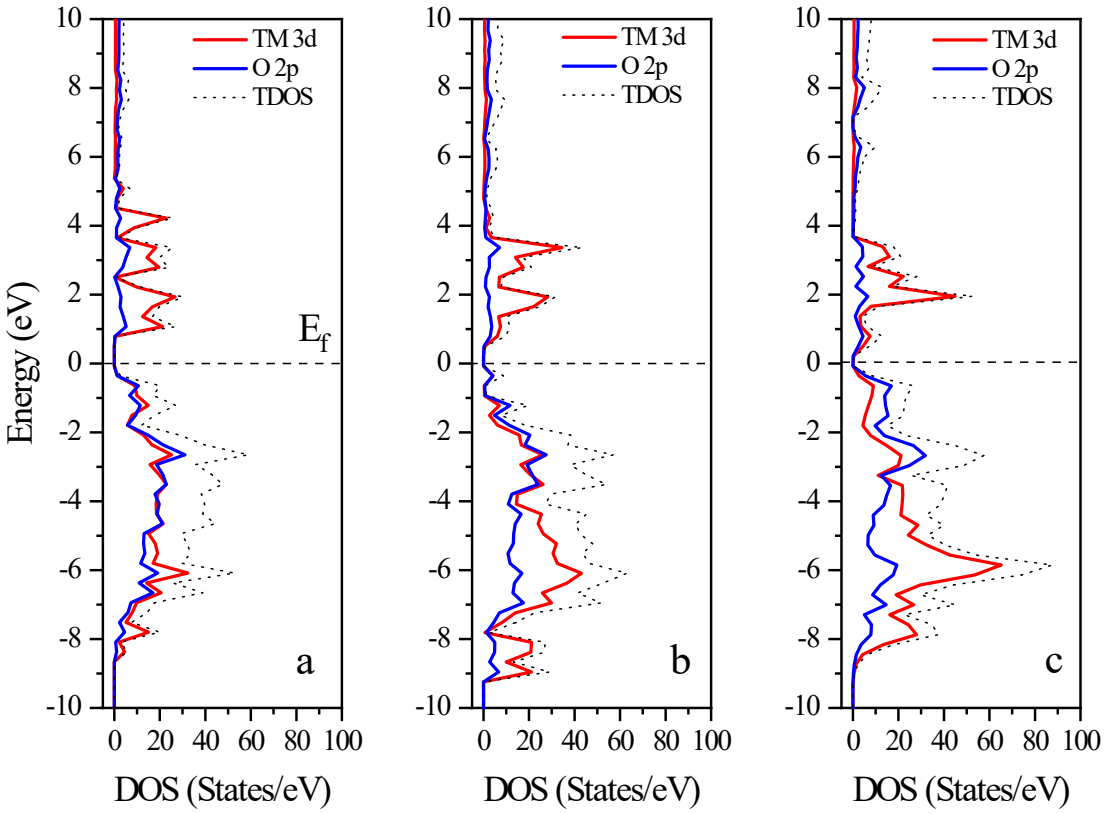

Fig. S7 The partial density of states (DOS) plots for a) FNZO, b) MFNZO and c) CMFNZO

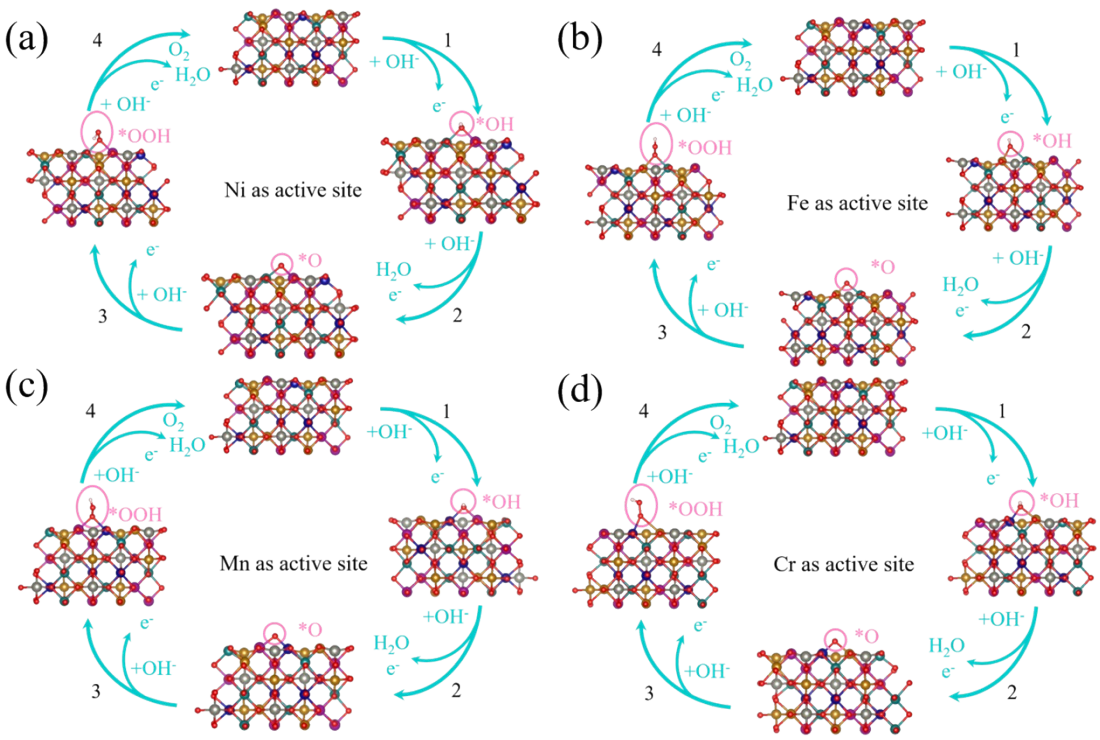

Fig. S8 The reaction pathway on different metal site for OER.

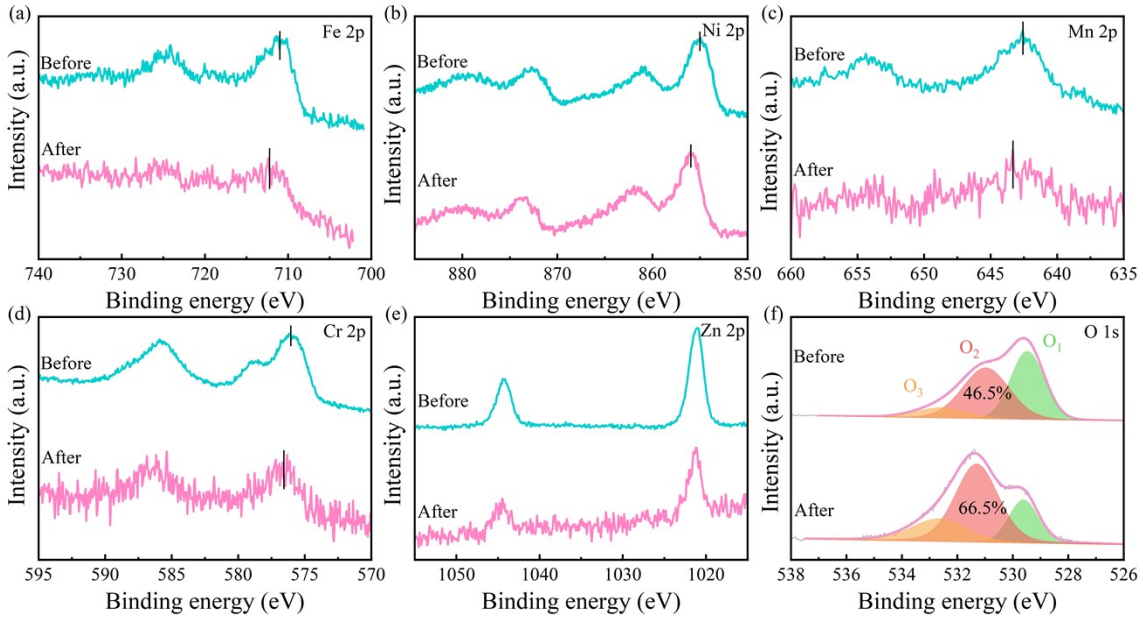

Fig. S9 XPS spectra of the CMFNZO before and after the stability test. (a) Fe 2p, (b) Ni 2p (c) Mn 2p (d) Cr 2p (e) Zn 2p and (f) O 1s.

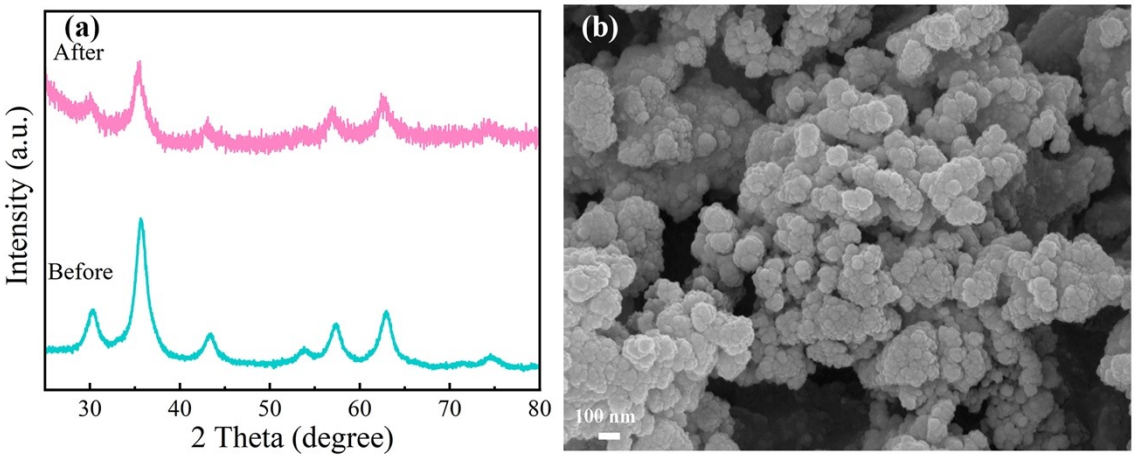

Fig. S10 (a) XRD pattern and (b) SEM image after the stability test of CMFNZO.

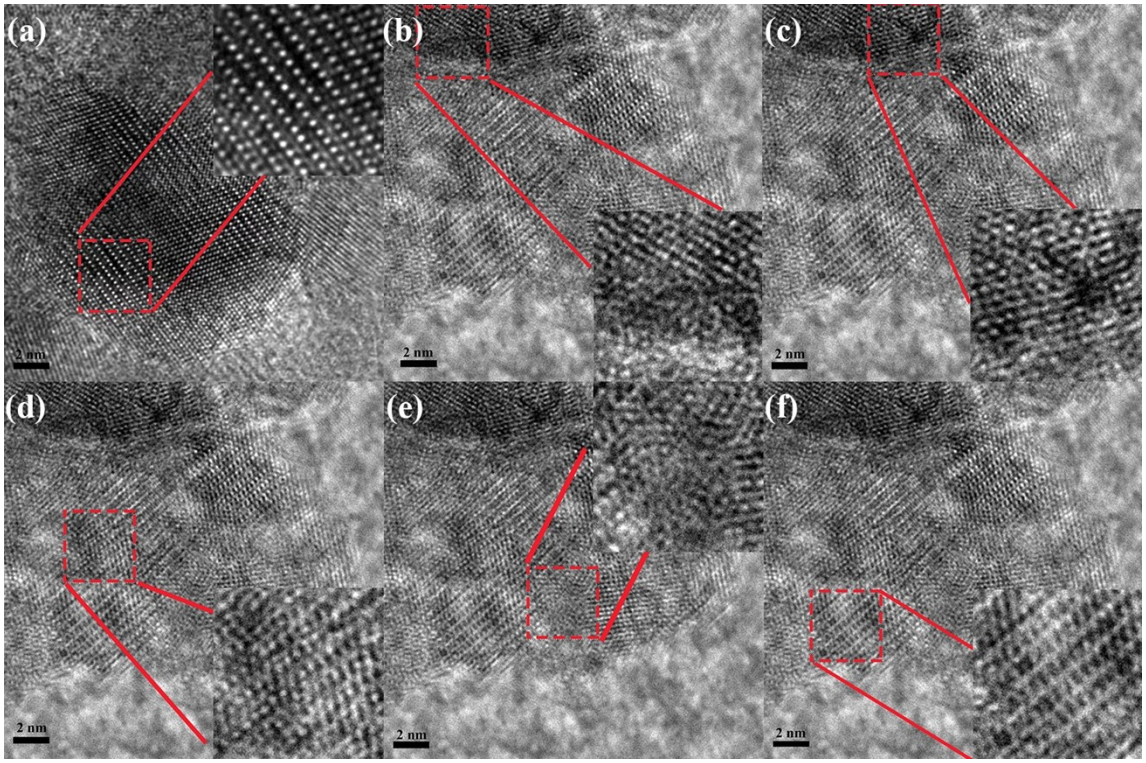

Fig. S11 The Fast Fourier Transform (FFT) patterns of the selected area in the corresponding HRTEM image of CMFNZO. (a) Before and (b-f) After the stability test.

After the stability test, the Fast Fourier transform (FFT) patterns of the different selected regions show the appearance of chaotic arrangements and missing atoms (Fig. S11b-f). As a comparison, the highly ordered arrangement of atoms is clearly observed in the sample before the stability test (Fig. S11a). The leaching of some elements (Cr, Mn and Zn) leads to the reduction of crystallinity of the material surface, creates a large number of lattice defects and possibly some kind of amorphization, which would facilitate the OER process.

Table S1. Crystal field stabilization energy (CFSE) of the selected elements

Ions	d^n	Tetrahedral (-*Dq*)	Octahedron (-*Dq*)
Cr^{3+}	d^3	3.56	12
Mn^{3+}	d^4	1.78	6
Fe^{3+}	d^5	0	0
Fe^{2+}	d^6	2.67	4
Ni^{3+}	d^7	5.34	8
Ni^{2+}	d^8	3.56	12
Zn^{2+}	d^{10}	0	0

Table S1 shows the CFSE values of selected elements with different valence at tetrahedron and octahedron positions, respectively.

The normal spinel $ZnFe_2O_4$ was modeled in a cubic frame with Fd-3m space group, consisting of eight zinc atoms, sixteen iron atoms and thirty-two oxygen atoms. In the structure, Zn^{2+} located at tetrahedral sites and Fe^{3+} settled on octahedral sites, respectively. The chemical formula can then be expressed as $(Zn_8)_{tetra}(Fe_{16})_{oct}O_{32}$. The high entropy spinel oxide model was established based on the perfect normal spinel $ZnFe_2O_4$ by replacing some Zn and Fe atoms with the doped elements. Based on the CFSE values, it is then proposed that for $(Fe_{0.33}Ni_{0.33}Zn_{0.33})_3O_4$, the chemical formula is $(Zn_8)_{tetra}(Fe_8Ni_8)_{oct}O_{32}$, and it is $(Zn_6Fe_2)_{tetra}(Fe_4Ni_6Mn_6)_{oct}O_{32}$ for $(Mn_{0.25}Fe_{0.25}Ni_{0.25}Zn_{0.25})_3O_4$, $(Zn_4Fe_4)_{tetra}(Fe_2Ni_6Mn_4Cr_4)_{oct}O_{32}$ for $(Cr_{0.2}Mn_{0.2}Fe_{0.2}Ni_{0.2}Zn_{0.2})_3O_4$.

As an example, the detail deduction to calculate the CFSE values for $(Mn_{0.25}Fe_{0.25}Ni_{0.25}Zn_{0.25})_3O_4$ is presented below:

If we suppose that all the Zn^{2+} and part of Fe^{3+} ions are located at tetrahedron position, the remaining elements are at octahedron positions, then based on the XPS analysis results (table 2), it is known that there are 6 Zn^{2+} and 2 Fe^{3+} at tetrahedron. The remaining 6 $Ni^{2+/3+}$, 6 Mn^{3+}, 3 Fe^{2+} and 1 Fe^{3+} ions are at octahedron position. Therefore the CFSE value could be calculated as: 6×0 (-*Dq*) + 2×0 (-*Dq*) + 2×12 (-*Dq*) + 4×8 (-*Dq*) + 6×6 (-*Dq*) + 3×4 (-*Dq*)+ 1×0 (-*Dq*) = -104 *Dq*

In the same way, if we suppose that part of Fe2+, Ni2+or Ni3+ at tetrahedron position, then the CFSE are -101.34 *Dq*, -87.12 *Dq* and -98.68 *Dq* . Considering that $(Zn_6Fe_2)_{tetra}(Fe_4Ni_6Mn_6)_{oct}O_{32}$ has the lowest CFSE value, it is then selected to model the crystal structure of $(Mn_{0.25}Fe_{0.25}Ni_{0.25}Zn_{0.25})_3O_4$.

Table S2. The configuration entropy of the samples.

Sample	S_{config}
CMFNZO	1.61R
MFNZO	1.39R
FNZO	1.10R
ZFO	0.64R

Table S3. ICP-OES analysis of the obtained samples.

Sample	Cr (ppm)	Mn (ppm)	Fe (ppm)	Ni (ppm)	Zn (ppm)
CMFNZO	9.251	7.920	12.15	11.72	11.49
MFNZO	0	11.66	17.82	16.25	17.27
FNZO	0	0	20.66	18.93	21.06
ZFO	0	0	38.33	0	20.29

Table S4. EIS fitting results of the multi-metal spinel oxides.

Sample	R_1 (Ω)	R_2 (Ω)
CMFNZO	8.74	21.75
MFNZO	12.51	27.81
FNZO	30.41	56.96
ZFO	2338	5194
RuO_2	11.66	41.62

Table S5. Element binding energy in MFNZO and FNZO.

Element	Oxidation Sate	MFNZO	FNZO
		$2p_{3/2}$ BE/eV	$2p_{3/2}$ BE/eV
Fe	Fe^{2+}	710.1	710.9
	Fe^{3+}	712.0	712.9
Ni	Ni^{2+}	855.1	854.6
	Ni^{3+}	856.9	855.8
Zn	Zn^{2+}	1021.3	1021.1
Mn	Mn^{3+}	642.1	---

Table S6. The proportion of Fe and Cr with different valence states in CMFNZO, MFNZO and FNZO.

Sample	Fe 2p		Cr 2p	
	Fe^{2+} (%)	Fe^{3+} (%)	Cr^{3+} (%)	Cr^{6+} (%)
CMFNZO	36.0 (23.0) *	64.0 (77.0) *	74.2 (82.7) *	25.8 (17.3) *
MFNZO	37.9	62.1	---	---
FNZO	41.7	58.3	---	---

*The values in the bracket are the analysis results of Fe and Cr after the OER measurement.

Table S7. Metal concentrations in 1M KOH electrolyte after long-term stability test.

Element	Concentration (ppm)
Cr	1.0450
Mn	0.3354
Fe	0.0963
Ni	0.0613
Zn	0.3262

Table S8. ICP-OES analysis of the CMFNZO before and after the long-term stability test.

Element	Before (molar %)	After (molar %)
Cr	19.0	11.0
Mn	16.0	22.0
Fe	24.0	22.0
Ni	22.0	24.0
Zn	19.0	21.0

Table S9. Comparison of OER activity of CMFNZO with the reported materials.

Electrocatalysts	Electrolyte	Overpotential at 10 mA cm^{-2} (mV)	Tafel slope (mV dec^{-1})	Ref.
$(CrMnFeNiZn)_3O_4$	1M KOH	295	53.7	This Work
$(CuCoMnFeNi)_3O_4$	1M KOH	400	76.7	[1]
HEO/MWCNT	1M KOH	350	59.5	[1]
$(CoMnFeNiZn)Fe_2O_4$	1M KOH	326	53.6	[2]
$(CoNiMnZnFe)_3O_{3.2}$	1M KOH	336	47.5	[3]
FeCoNiMnBOx	1M KOH	266	64.5	[4]
FeCoNiCuBOx	1M KOH	264	73.9	[4]
FeCoNiSnBOx	1M KOH	258	68.2	[4]
(MgFeCoNiCu)Ox	1M KOH	300	40.0	[5]
$La(CrMnFeCo_2Ni)O_3$	1M KOH	325	51.2	[6]
$NiCo_{2-x}Fe_xO_4$	1M KOH	272	42.0	[7]
Co_3O_4 nanotubes	1M KOH	390	76.0	[8]
Fe-doped Co_3O_4	1M KOH	380	60.0	[9]
Co_3O_4/Co-Fe oxide	1M KOH	297	61.0	[10]
Zn-doped $NiCo_2O_4$	1M KOH	560	62.0	[11]

References：

[1] D. D. Wang, Z. J. Liu, S. Q. Du, Y. Q. Zhang, H. Li, Z. H. Xiao, W. Chen, R. Chen, Y. Y. Wang, Y. Zou and S. Y. Wang, *J. Mater. Chem. A*, 2019, **7**, 24211-24216.
[2] Y. Zhang, T. Lu, Y. K. Ye, W. J. Dai, Y. A. Zhu and Y. Pan, *ACS Appl. Mater. Interfaces*, 2020, **12**, 32548-32555.
[3] Y. Zhang, W. J. Dai, P. F. Zhang, T. Lu and Y. Pan, *J. Alloys Compd.*, 2021, **868**, 159064.
[4] S. D. Jiang, K. H. Tian, X. L. Li, C. Duan, D. Wang, Z. Wang, H. Sun, R. G. Zheng, and Y. G. Liu, *J. Colloid Interface Sci.*, 2022, **606**, 635-644.
[5] T. X. Nguyen, Z. T. Huang and J. M. Ting, *Appl. Surf. Sci.*, 2021, **570**, 151160.
[6] T. X. Nguyen, Y. C. Liao, C. C. Lin, Y. H. Su and J. M. Ting, *Adv. Funct. Mater.*, 2021, **31**, 2101632.
[7] Y. Huang, S. L. Zhang, X. F. Lu, Z. P. Wu, D. Y. Luan and X. W. Lou, *Angew. Chem. Int. Ed.*, 2021, **60**, 11841-11846.
[8] H. Wang, S. F. Zhuo, Y. Liang, X. L. Han and B. Zhang, *Angew. Chem. Int. Ed.*, 2016, **128**, 9201-9205.
[9] C. L. Xiao, X. L. Lu and C. Zhao, *Chem. Commun.*, 2014, **50**, 10122-10125.
[10] X. Wang, L. Yu, B. Y. Guan, S. Y. Song and X. W. Lou, *Adv. Mater.*, 2018, **30**, 1801211.
[11] M. Yang, Y. F. Li, Y. Yu, X. C. Liu, Z. Shi and Y. Xing, *Chem. Eur. J.*, 2018, **24**, 13002-13008.